iScience

Article

Spatiotemporal profiling of protein kinase A activity in spontaneously beating hiPSC-derived cardiac organoids

Graphical abstract

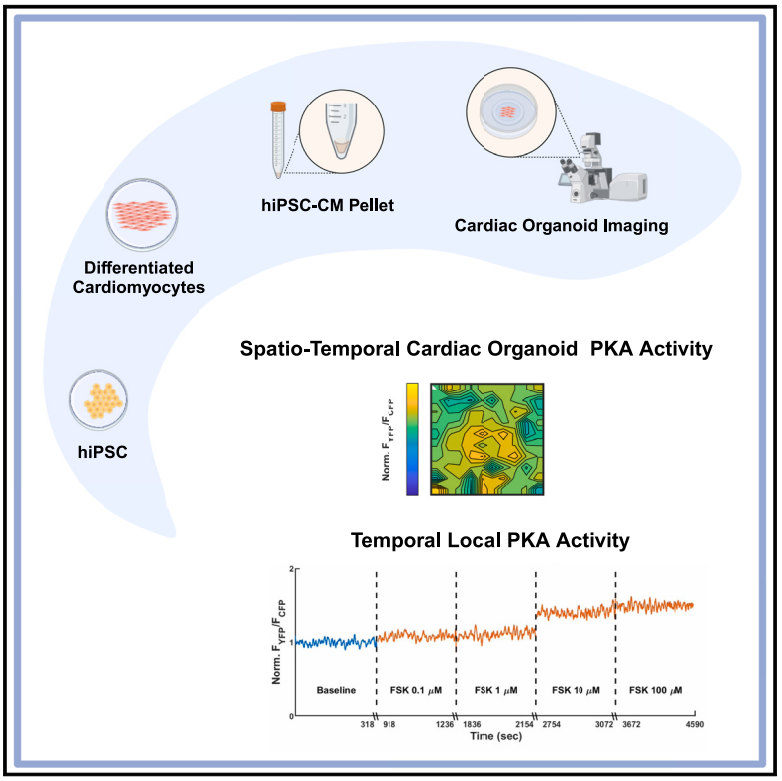

Highlights

- We introduce spatiotemporal measurement of PKA activity in cardiac organoids
- Cardiac organoids exhibit robust and spatially heterogeneous PKA activity
- PKA activity stimulants induce greater spatial heterogeneity compared to inhibitors

Authors

Ido Weiser-Bitoun, Savyon Mazgaoker, Rami Eid, Inbar Brosh, Yael Yaniv

Correspondence

yaely@bm.technion.ac.il

In brief

Natural sciences; Biological sciences; Cell biology; Stem cells research

Weiser-Bitoun et al., 2025, iScience *28*, 112005
March 21, 2025
https://doi.org/10.1016/j.isci.2025.112005

CellPress

iScience

CellPress
OPEN ACCESS

Article

Spatiotemporal profiling of protein kinase A activity in spontaneously beating hiPSC-derived cardiac organoids

Ido Weiser-Bitoun,[1,2,3] Savyon Mazgaoker,[1] Rami Eid,[1] Inbar Brosh,[1] and Yael Yaniv[1,4,*]

[1]Laboratory of Bioelectric and Bioenergetic Systems, Faculty of Biomedical Engineering, Technion-Israel Institute of Technology, Haifa 3200003, Israel

[2]Rappaport Faculty of Medicine, Technion-Israel Institute of Technology, Haifa 3525433, Israel

[3]Department of Internal Medicine "C", Rambam Health Care Campus, Haifa 3109601, Israel

[4]Lead contact

*Correspondence: yaely@bm.technion.ac.il

https://doi.org/10.1016/j.isci.2025.112005

SUMMARY

Protein kinase A (PKA) phosphorylates proteins crucial for rhythm modulation, with its dysregulation linked to arrhythmias. This study investigated PKA activity's spatiotemporal dynamics in spontaneously beating cardiac organoids. We hypothesized that PKA activity would respond to autonomic stimulation and exhibit spatial heterogeneity upon drug-induced modulation. Forskolin (activator) and H-89 (inhibitor) altered PKA activity ratios from 1 to 1.52 ± 0.03 and 0.89 ± 0.03, respectively. Hill equation-based regression showed a high fit of PKA activity behavior for all four tested drugs (forskolin, H-89, isoproterenol, or carbachol) at concentrations. Responses to forskolin or isoproterenol, which increase PKA activity, showed higher heterogeneity (10.1 ± 0.8% or 8.7 ± 1%) compared to responses to H-89 or carbachol (4.3 ± 0.8% or 4.4 ± 1.2%), which decrease PKA activity. These results reveal the intricate spatial dynamics of PKA activity in cardiac organoids and its dependence on PKA activation levels.

INTRODUCTION

Cardiac tissue serves as a crucial model for studying heart function and dysfunction, particularly as arrhythmias arise from disturbances in the electrical propagation across cells. In this context, cardiac organoids derived from human induced pluripotent stem cells (hiPSCs) stand out as a superior human model of heart tissue.[1] The organoids are used to gain insights into the mechanisms that initiate and propagate electrical activity across a wide range of sinus rhythms. Such knowledge constitutes the initial step toward understanding how alterations in these mechanisms can ultimately lead to arrhythmias.

The body-wide neuro-visceral axes play a role in controlling heart rate through the dual activation of sympathetic and parasympathetic pathways, which, in turn, modulate cardiomyocyte (CM) activity. Specifically, activation of β-adrenergic receptors (β-AR) on the cell membrane triggers G-coupled proteins, subsequently activating adenylate cyclase (AC). AC, in turn, catalyzes the conversion of ATP to cAMP, leading to activation of protein kinase A (PKA) and to increased cellular activity in CMs. In contrast, activation of muscarinic receptors on the CM membrane triggers G-inhibitory proteins that reduce AC and PKA activities.[2]

In cardiac cells, PKA plays a pivotal role in supporting the phosphorylation of key proteins associated with modulation of the beating rate (Figure 1A). These proteins include ion channels located on the cellular membrane (e.g., funny-current channel and L-type channel) or on the sarcoplasmic reticulum (SR, such as the ryanodine receptor) membrane, SR proteins (e.g., phospholamban), sarcomere proteins (including troponin and myosin-binding protein-C), and transcription factors (e.g., cAMP-response element-binding protein [CREB]).[3] This multifaceted list of targets underscores the significance of PKA as a key regulator of various aspects of cellular function and contractility.

PKA activity has been documented in single atrial, ventricular, and sinoatrial node cells[4–7] and has been investigated in single hiPSC-derived CMs.[8] However, its spatiotemporal activity in cardiac organoids or cardiac tissue has not been reported. These complex three-dimensional structures showed clear sarcomere formation (Figure S1) and propagation of electrical activity (Figure S2), and could provide a more physiologically relevant context as compared to single cells, for investigation of PKA dynamics and the underlying regulatory mechanisms.

The current work aimed to measure PKA activity in cardiac organoids (Table S1) and to examine its spatiotemporal characteristics under basal conditions as well as in response to β-adrenergic and cholinergic stimulation. First, we hypothesize that PKA activity will be influenced by sympathetic and parasympathetic stimulation, resulting in spatial distribution. Second, we posit that cardiac organoid responses to drugs that either elevate or reduce PKA activity will induce spatial PKA heterogeneity. To

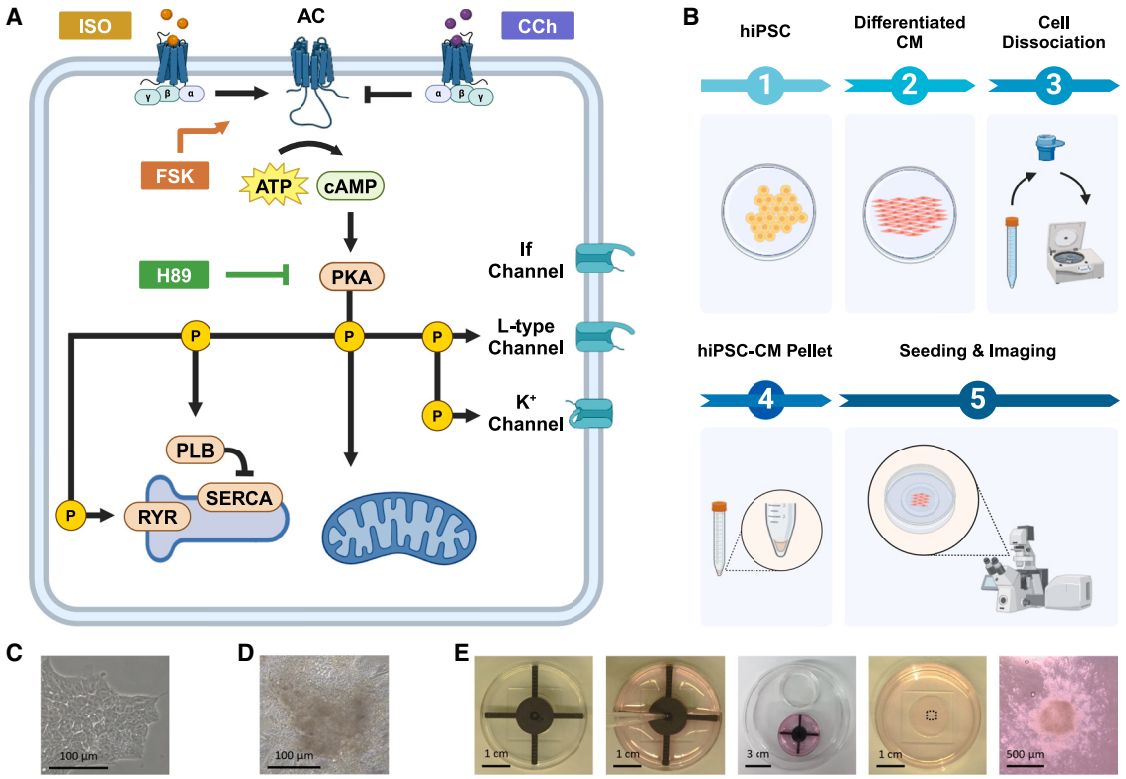

Figure 1. Experimental method to measure PKA in spontaneously beating cardiac organoid

(A) Schematic illustration of AC-cAMP/PKA cascade in cardiomyocytes: This schematic illustrates the cellular targets of the four tested drugs—forskolin (FSK), H-89, isoproterenol (ISO), and carbachol (CCh). ISO activates adrenergic receptors, subsequently stimulating adenylate cyclase (AC). AC, in turn, catalyzes the conversion of ATP to cAMP, leading to the activation of protein kinase A (PKA). cAMP activated the funny channel. PKA then phosphorylates targets associated with increases in beating rate, such as phospholamban (PLB) and ryanodine receptor (RyR) on the sarco-endoplasmic reticulum calcium ATPase (SERCA). CCh activates muscarinic receptors, inhibiting AC. FSK directly activates AC, while H-89 directly inhibits PKA.

(B) Schematic of the steps involved in generation of spontaneously beating cardiac organoids. Human induced pluripotent stem cells (hiPSCs) are differentiated into cardiomyocytes (CMs), which are then dissociated and centrifuged. The cell pellet is seeded on dishes for confocal microscope observation.

(C) Image of hiPSC culture.

(D) Image of CMs differentiated from hiPSCs.

(E) Cardiac organoid formed process: CMs are seeded onto Matrigel-coated dishes using a seeding-guide ring with a 1 mm^2 hole to focus cell seeding. Plates are incubated at 37°C in a 5% CO_2 incubator within a humidified large Petri dish. After 6–7 days, spontaneously beating cardiac organoids are imaged. Scale bars are indicated on each image.

this end, the spatiotemporal activity of PKA in cardiac organoids (Figures 1B–1E) exposed to substrates that enhance (forskolin, an AC activator, or isoproterenol, an adrenergic agonist) or suppress (H-89, a direct PKA inhibitor, or carbachol, a muscarinic agonist) PKA activity (Figure 1A) was measured.

RESULTS

The effect of an AC agonist on PKA activity in spontaneously beating cardiac organoids

To determine the dynamic range of PKA activity, its levels were first elevated by exposing cardiac organoids to increased concentrations of forskolin (0.1–100 μM), an established AC agonist. Figure 2A displays a heatmap of the averaged, normalized steady-state yellow fluorescent protein (YFP)/cyan fluorescent protein (CFP) signal over time for each drug concentration in a representative cardiac organoid. From the region marked by the red square in Figure 2A, we extracted the local normalized YFP/CFP signals over time, which are presented in Figure 2B. Video S1 exhibits the heatmap of the normalized YFP/CFP signal over time, including the local normalized YFP/CFP fluorescent signal from the same organoid shown in Figures 2A and 2B, with the corresponding location marked by the red square.

The mean local normalized YFP/CFP signal exhibited a dose-dependent increase from baseline in the presence of escalating concentrations of forskolin, reaching a maximal mean increase of 52.4 ± 3.3% in response to 100 μM of the drug (Figure 2C).

To confirm that forskolin indeed increases PKA activity, cardiac organoids were immunostaining for phosphorylated phospholamban. As expected, staining intensity was increased in the presence of forskolin (Figures S3 and S4).

Additionally, we validated the stability of the YFP/CFP signal by measuring blank (baseline) samples over seven measurements

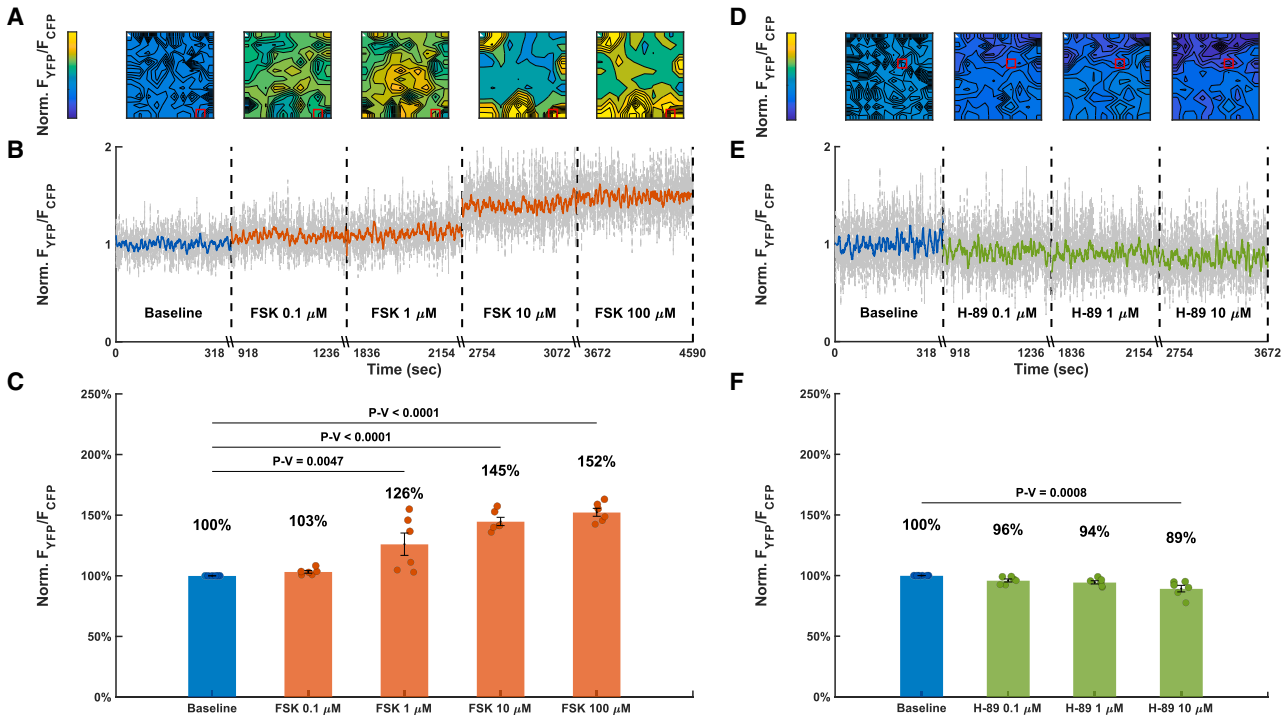

Figure 2. PKA activity in spontaneously beating cardiac organoids in response to forskolin or H-89

(A) Averaged normalized steady-state YFP/CFP signal over time for each tested forskolin (FSK) concentration (0.1–100 μM) in a representative cardiac organoid.

(B) Representative example of local normalized YFP/CFP signal over time, displayed for one location (red square) measured from the same cardiac organoid presented in (A), for each FSK concentration.

(C) Mean local normalized YFP/CFP signal derived from six cardiac organoids at each FSK concentration, obtained from three separate hiPSC differentiations to CMs.

(D) Averaged normalized steady-state YFP/CFP signal over time for each tested H-89 concentration (0.1–10 μM) in a representative cardiac organoid.

(E) Representative example of local normalized YFP/CFP signal over time, displayed for one location (red square) measured from the same cardiac organoid presented in (D), for each H-89 concentration.

(F) Mean local normalized YFP/CFP signal, derived from six cardiac organoids for each tested H-89 concentration, obtained from four separate hiPSC differentiations to CMs.

Data are presented as mean ± SE, and statistical comparison was performed using one-way analysis of variance.

(representing the maximum number of steps used for substance measurements), as illustrated in Figure S5.

The effect of a PKA inhibitor on PKA activity in spontaneously beating cardiac organoids

To assess the reduction in PKA activity, cardiac organoids were exposed to increasing concentrations of H-89 (ranging from 0.1 to 10 μM), a direct PKA inhibitor. Figure 2D displays a heatmap of the averaged, normalized steady-state YFP/CFP signal over time for each drug concentration in a representative cardiac organoid. From the region marked by the red square in Figure 2D, we extracted the local normalized YFP/CFP signals over time are presented in Figure 2E. Video S2 showcases the heatmap of the normalized YFP/CFP fluorescent signal over time, including the local normalized YFP/CFP fluorescent signal from the same organoid shown in Figures 2D and 2E, with the corresponding location marked by the red square.

The mean local normalized YFP/CFP signal exhibited a dose-dependent decrease from baseline in the presence of escalating concentrations of H-89, reaching a maximal mean decrease of 10.8 ± 2.7% in response to 10 μM of the drug (Figure 2F).

To confirm that H-89 indeed decreased PKA activity, cardiac organoids were immunostaining for phosphorylated phospholamban. As expected, staining intensity was lower in the presence of H-89 (Figures S3 and S4).

The effect of sympathetic stimulation on PKA activity in spontaneously beating cardiac organoids

To assess cardiac organoid PKA activity under sympathetic stimulation, samples were exposed to elevated concentrations of isoproterenol (ranging from 1 to 1,000 nM), a β-adrenergic agonist. Figure 3A displays a heatmap of the averaged, normalized steady-state YFP/CFP signal over time for each drug concentration in a representative cardiac organoid. From the region marked by the red square in Figure 3A, we extracted the local normalized YFP/CFP signals over time are presented in Figure 3B. Video S3 showcases the heatmap of the normalized YFP/CFP fluorescent signal over time,

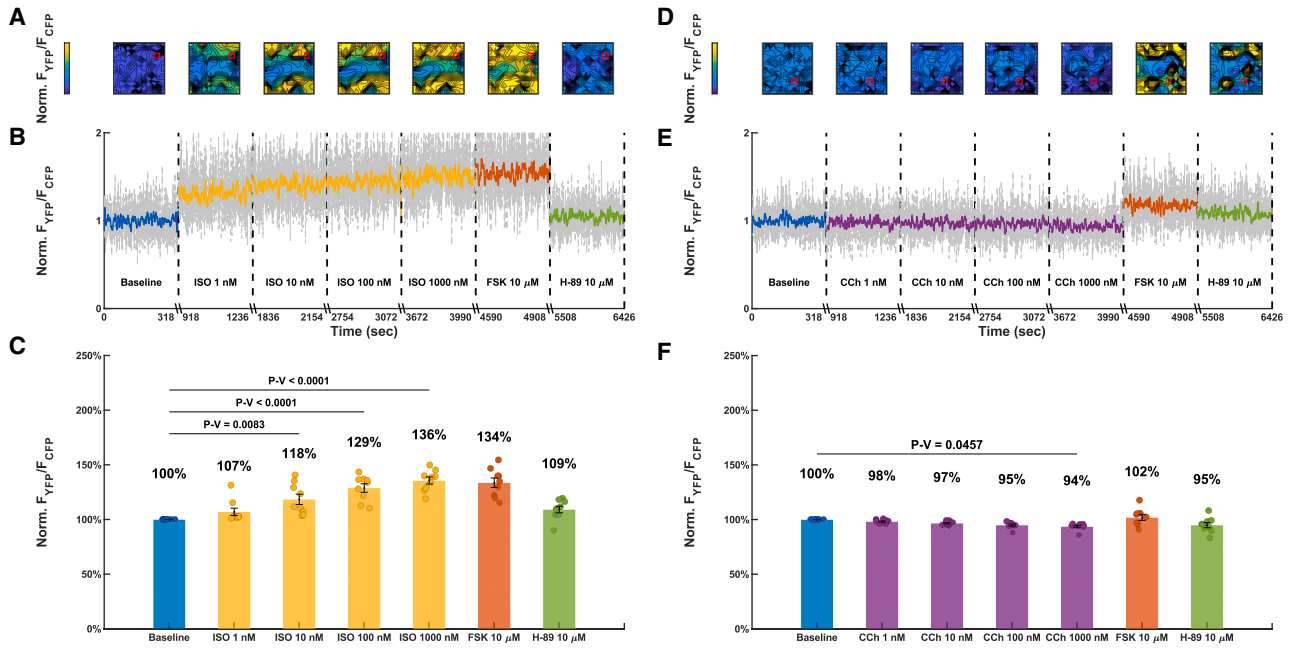

Figure 3. PKA activity of spontaneously beating cardiac organoids in response to sympathetic or para-sympathetic stimulation

(A) Averaged normalized steady-state YFP/CFP signal over time at each tested isoproterenol (ISO) concentration (1–1,000 nM), in a representative cardiac organoid.

(B) Representative example of local normalized YFP/CFP signal over time, displayed for one location (red square) measured from the same cardiac organoid presented in (A), for each ISO concentration, followed by treatment with 10 μM forskolin and H-89.

(C) Mean local normalized YFP/CFP fluorescent signal, derived from nine cardiac organoids for each tested ISO concentration followed by treatment with 10 μM forskolin and H-89, obtained from five separate hiPSC differentiations to CMs.

(D) Averaged normalized steady-state YFP/CFP signal over time for each tested CCh concentration (1–1,000 nM) in a representative cardiac organoid.

(E) Representative example of local normalized YFP/CFP signal over time, displayed for one location (red square) measured from the same cardiac organoid presented in (D) for each tested CCh concentration followed by treatment with 10 μM forskolin and H-89.

(F) Mean local normalized YFP/CFP signal, derived from nine cardiac organoids for each tested CCh concentration, obtained from four separate hiPSC differentiations to CMs.

Data are presented as mean ± SE, and statistical comparison was performed using one-way analysis of variance.

including the local normalized YFP/CFP fluorescent signal from the same organoid shown in Figures 3A and 3B, with the corresponding location marked by the red square. The mean local normalized YFP/CFP signal exhibited a dose-dependent increase from baseline in the presence of escalating concentrations of isoproterenol, reaching a maximal mean increase of 35.7% ± 3.2% in response to 1,000 nM of the drug (Figure 3C).

At the end of the measurements, both forskolin and H-89 were applied to determine the dynamic range of PKA activity. On average, forskolin did not further increase PKA activity (33.6 ± 4.3% increase relative to baseline), while H-89 decreased the signal to 9.2 ± 3% above baseline.

The effect of parasympathetic stimulation on PKA activity in spontaneously beating cardiac organoids

To assess cardiac organoid PKA activity under parasympathetic stimulation, cardiac organoids were exposed to elevated concentrations of carbachol (1–1,000 nM), a muscarinic agonist. Figure 3D displays a heatmap of the averaged, normalized steady-state YFP/CFP signal over time for each drug concentration in a representative cardiac organoid. From the region marked by the red square in Figure 3D, we extracted the local normalized YFP/CFP signals over time are presented in Figure 3E. Video S4 showcases the heatmap of the normalized YFP/CFP fluorescent signal over time, including the local normalized YFP/CFP fluorescent signal from the same organoid shown in Figures 3D and 3E, with the corresponding location marked by the red square.

The mean local normalized YFP/CFP signal exhibited a dose-dependent decrease from baseline in the presence of escalating concentrations of carbachol, reaching a maximal mean decrease of 6.4% ± 1.0% below baseline under a carbachol concentration of 1,000 nM (Figure 3F).

At the end of the measurements, both forskolin and H-89 were applied to determine PKA dynamics. On average, forskolin increased PKA activity to 101.9 ± 2.6% relative to baseline, while H-89 decreased it to 94.9 ± 2.3%.

Correlation between PKA activity and drug concentration

To characterize the dynamics of cardiac organoid PKA activity in response to physiological and pharmacological perturbations, the trend of its response to each of the four tested drugs

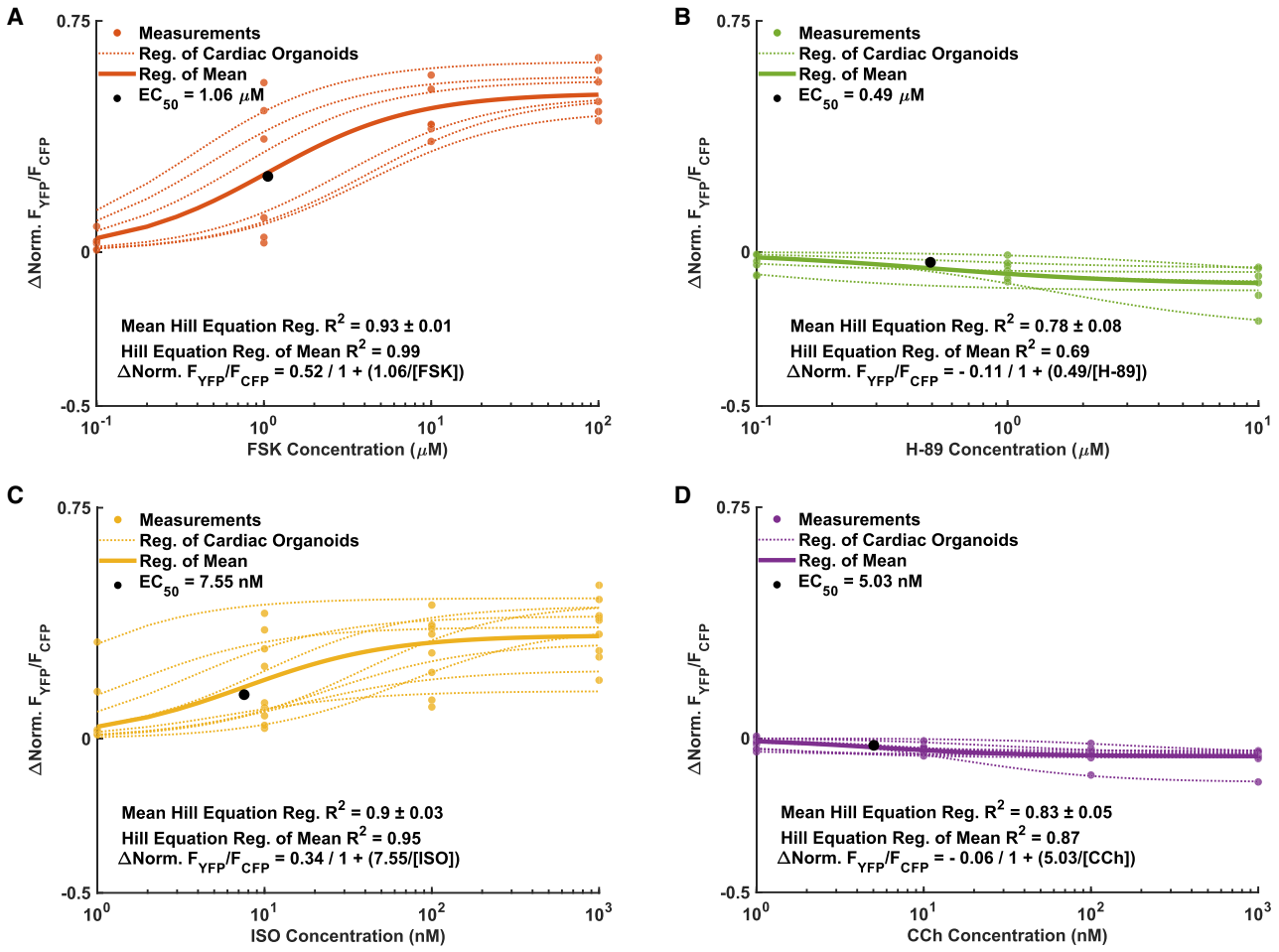

Figure 4. PKA activity measurement regression of Hill equation

(A) Forskolin (FSK) Hill equation regression: normalized YFP/CFP signal of all six cardiac organoids versus FSK concentration, along with regression of the mean fluorescent signal. EC_{50} is marked by a black dot.

(B) H-89 Hill equation regression: normalized YFP/CFP signal of all six cardiac organoids versus H-89 concentration, and regression of the mean fluorescent signal. EC_{50} is marked by a black dot.

(C) Isoproterenol (ISO) Hill equation regression: normalized YFP/CFP signal of all nine cardiac organoids versus ISO concentration, along with regression of the mean fluorescent signal. EC_{50} is marked by a black dot.

(D) Carbachol (CCh) Hill equation regression: normalized YFP/CFP signal of all nine cardiac organoids versus CCh concentration, and regression of the mean fluorescent signal. EC_{50} is marked by a black dot.

(forskolin, H-89, isoproterenol, or carbachol) was analyzed. A tight R^2 was obtained for the regression of the mean fluorescent signal for all organoids versus forskolin concentration (0.99), as well as for the regression of each organoid (0.93 ± 0.01) (Figure 4A). The R^2 for the regression of the mean fluorescent signal of all organoids versus H-89 concentration was 0.69, and the mean R^2 for the regression of each organoid was 0.78 ± 0.08 (Figure 4B). Similarly, a tight R^2 for the regression of the mean fluorescent signal of all organoids versus isoproterenol concentration (0.95) was obtained, along with a tight mean R^2 for the regression of each organoid (0.9 ± 0.03) (Figure 4C). A tight R^2 was also noted for the regression of the mean fluorescent signal of all organoids versus carbachol concentration (0.87), as well as for the regression of each organoid (0.83 ± 0.05) (Figure 4D).

Spatial modulation of PKA activity by the AC-cAMP/PKA cascade

To explore the spatial distribution of PKA activity of cardiac organoids, its levels at different locations were measured in the basal state and in response to four drugs affecting the AC-cAMP/PKA cascade. Organoids were divided into 100 regions. Only locations with a positive normalized YFP/CFP signal response to one of the applied drugs (i.e., an increase in signal from baseline to the response for 10 μM forskolin or 1,000 nM isoproterenol or a decrease in signal from baseline to the response for 10 μM H-89 or 1,000 nM carbachol) were included in the analysis. Figures 5A–5D show different local normalized YFP/CFP signal at each four regions in the cardiac organoids shown in Figures 2A, 2D, 3A, and 3D, respectively, that were subsequently exposed to either forskolin, H-89, isoproterenol, or carbachol,

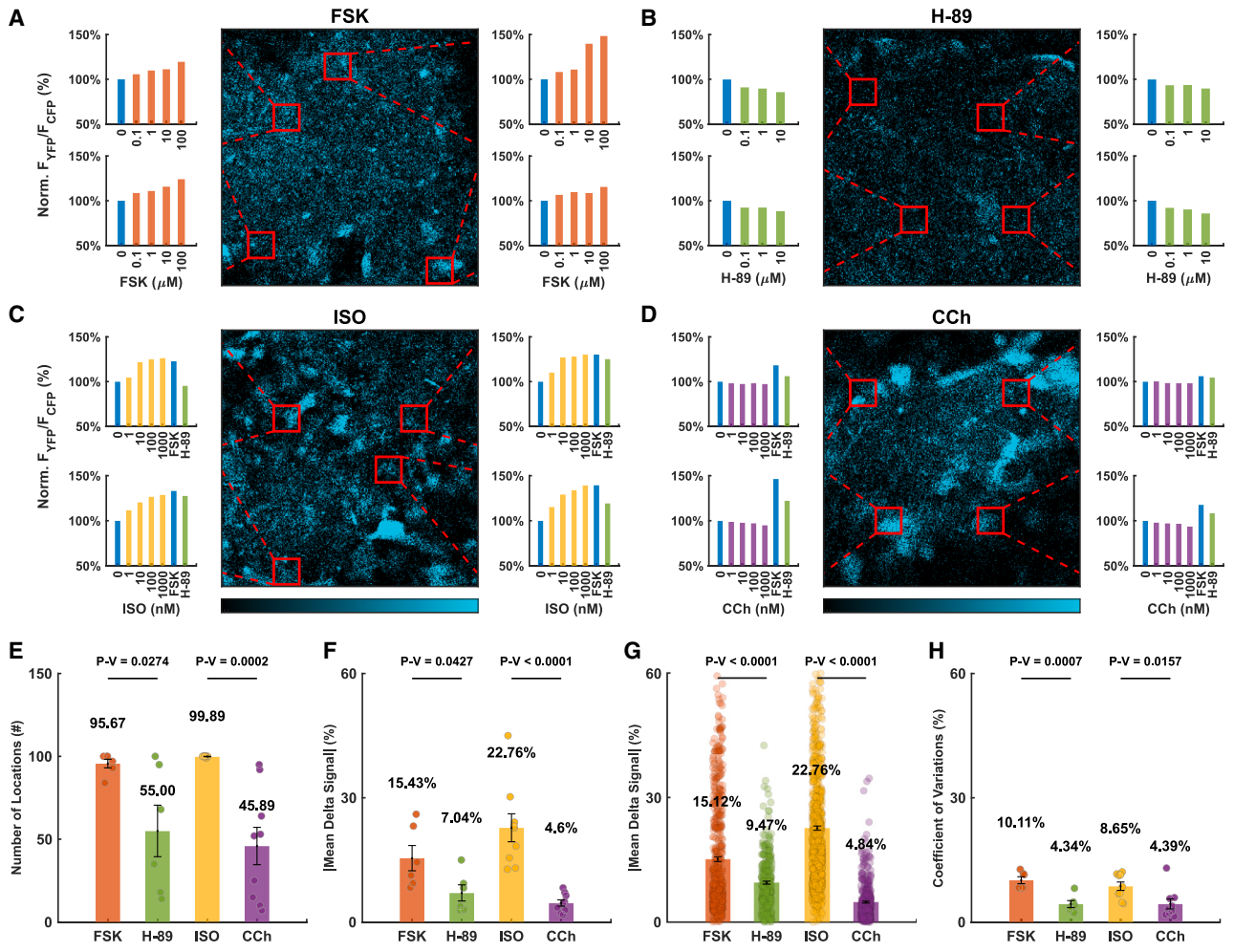

Figure 5. Spatial analysis of PKA activity in response to AC-cAMP/PKA cascade modulation

(A) Local normalized YFP/CFP signals at four locations in a representative cardiac organoid (as in Figure 2A) following treatment with 0.1–100 μM forskolin (FSK).

(B) Local normalized YFP/CFP signals at four locations in a representative cardiac organoid (as in Figure 2D) following treatment with 0.1–10 μM H-89.

(C) Local normalized YFP/CFP signals at four locations in a representative cardiac organoid (as in Figure 3A) following treatment with 1–1,000 nM isoproterenol (ISO), followed by 10 μM FSK and H-89.

(D) Local normalized YFP/CFP signals at four locations in a representative cardiac organoid (as in Figure 3D) following treatment with 1–1,000 nM carbachol (CCh), followed by 10 μM FSK and H-89. Color limits were adjusted for optimal visualization.

(E) Mean averaged number of positive response locations: positive responses determined by signal increase or decrease between baseline vs. following treatment with 10 μM FSK and H-89, respectively, and between baseline vs. following treatment with 1,000 nM isoproterenol and CCh, respectively.

(F) Absolute value of mean averaged normalized YFP/CFP signal, relative to baseline of all positive response locations for each cardiac organoid in response to FSK, H-89, isoproterenol, and CCh.

(G) Absolute value of mean normalized YFP/CFP signal, relative to baseline for all locations in all cardiac organoids positively responding to FSK, H-89, isoproterenol, or CCh.

(H) Mean averaged coefficient of variations: standard error divided by the average of the normalized YFP/CFP signal relative to baseline for all locations for each cardiac organoid positively responding to FSK, H-89, isoproterenol, or CCh. *p* values were calculated using a two-sided t test.

respectively. Figure 5E presents the mean averaged number of regions per organoid with a positive response to any of the four drugs. For forskolin and isoproterenol, nearly all regions exhibited a positive response to these substances (95.7 ± 2.6 and 99.9 ± 0.1 regions, respectively). In contrast, only approximately half of the regions positively responded to H-89 or carbachol (55 ± 15.5 and 45.9 ± 11.3 regions, respectively). Figure 5F illustrates the mean averaged normalized YFP/CFP signal relative to baseline for all positively responding regions per cardiac organoid. The response to forskolin was 2-fold higher than to H-89 (15.4 ± 3% increase relative to a 7 ± 2% decrease, respectively), and the response to isoproterenol was almost 5-fold higher than to carbachol (22.8 ± 3.4% increase relative to a 4.6 ± 0.8% decrease, respectively). Figure 5G shows the mean normalized YFP/CFP signal relative to baseline for all positively responding regions in all cardiac organoids. Similar results were found for

all four drugs (15.1 ± 0.6%, 9.5 ± 0.4%, 22.8 ± 0.5%, and 4.8 ± 0.2% for forskolin, H-89, isoproterenol, and carbachol, respectively), as observed in the mean averaged results. Figure 5H presents the mean averaged coefficient of variations of the normalized YFP/CFP signal relative to baseline for all positive regions per cardiac organoid. Relatively high coefficients were calculated for forskolin and isoproterenol (10.1 ± 0.8% and 8.7 ± 1%, respectively) and low coefficients for H-89 and carbachol (4.3 ± 0.8% and 4.4 ± 1.2%, respectively).

DISCUSSION

Main findings

The present study investigated the spatiotemporal dynamics of PKA activity in cardiac organoids. When exposed to drugs that either activate or deactivate PKA signaling, organoids show robust and spatially heterogenous PKA activity, consistent with our initial hypothesis. There was a higher spatial distribution of PKA activity in response to stimulants as compared to inhibitors of PKA. This finding supports our second hypothesis, indicating that the cardiac organoid's response to drugs, whether enhancing or reducing PKA activity, leads to spatial PKA heterogeneity.

1D and 2D PKA activity measurement in spontaneously beating cardiac organoids

FRET-based measurements of PKA activity in spontaneously beating cardiac organoids were analyzed in two ways. One-dimensional (1D) analysis examined the same location in the cardiac organoid over time, both at baseline and in response to increased substance concentrations. This provided a dynamic understanding of PKA activity at a specific location. The two-dimensional (2D) analysis inspected all regions of the cardiac organoid both at baseline and in response to each substance concentration separately. The results were presented as an averaged heatmap and as heatmaps over time, offering a comprehensive view of the spatial and temporal aspects of PKA activity. Notably, all experiments were conducted without pacing, to ensure that the spontaneous electrophysiological activity of the cells was not overdriven. This comprehensive approach provided valuable insights into the complex interplay between spatial and temporal dynamics of PKA activity.

PKA activity in response to drugs that affect AC-cAMP/PKA cascade

The PKA activity of spontaneously beating cardiac organoids was assessed in the presence of forskolin and H-89, two direct manipulators of the AC-cAMP/PKA signaling pathway. A significant increase in PKA activity was observed in response to forskolin, reaching a relatively higher magnitude with more area in the organoid that response. In comparison, a decrease in PKA activity observed in response to H-89, smaller in relative magnitude to forskolin with less area in the organoid that response. The relative higher increase in PKA activity may be indicative of a rapid response to the activation of AC by forskolin, which then leads to an elevation in cAMP levels and Ca^{2+}, resulting in degradation of phosphodiesterases and phosphatases. Alternatively, the observed pattern may imply relatively low basal PKA activity in the spontaneously beating cardiac organoids. The relative high increase could be the result of forskolin-induced AC activation to overcome the low baseline PKA activity, while the subsequent decline may suggest a regulatory mechanism to restore PKA activity to its basal state. Further investigations are warranted to delineate the specific contributions of phosphodiesterases, phosphatases and baseline PKA activity to cardiac organoid responses to perturbations in AC-cAMP/PKA signaling. Figures S3 and S4 confirm that immunostaining for phosphorylated phospholamban revealed an increase or decrease in phospholamban phosphorylation in response to forskolin or H-89, respectively. While the organoid margins tend to exhibit higher signals than the center, we accounted for this phenomenon by comparing the normalized PKA activity across different locations.

PKA activity under sympathetic and parasympathetic stimulation

The PKA activity of spontaneously beating cardiac organoids was also assessed in the presence of isoproterenol and carbachol, representing sympathetic and parasympathetic stimulation, respectively. In alignment with the observations relating to drugs that affect AC-cAMP/PKA cascade, the effects of these drugs on PKA activity did not manifest in the same absolute value levels. Specifically, a significant and relatively higher-magnitude increase in PKA activity was measured in response to all doses of isoproterenol compared to the magnitude of the decrease in PKA activity observed in response to carbachol. The higher potency of isoproterenol may, in addition to the aforementioned interpretations for forskolin, be attributed to the greater activation of adrenergic receptors compared to muscarinic receptors. Interestingly, the expression level of the muscarinic acetylcholine receptor M2-4 in hiPSCs (activated by carbachol) was similar to that of the β1 and β2 adrenergic receptors.[9] However, similar to the trends observed for PKA, a relatively greater increase in beating rate was measured in response to all doses of isoproterenol compared to the decrease in beating rate observed with carbachol.[10] The correlation between AC-cAMP/PKA cascade activity and the spontaneous beating rate of hiPSCs that was reported before[8] supports our finding that PKA activation has a greater effect than inhibition.

Regression of dose-response measurements

Regression based on Hill equation models achieved a high fit of PKA behavior in cardiac organoids for all explored drug concentrations. A non-linear relationship was observed, akin to the logarithmic relation observed between cAMP and elevated concentrations of forskolin (1 nM–100 μM) in hiPSC-CM spheroids.[11]

In PC12D cells (adrenal medulla pheochromocytoma cell line), H-89 with a reported Ki of 0.05 ± 0.01 μM,[12] was initially used as an inhibitor of cAMP-dependent protein kinases. However, an ED_{50} of 0.49 μM for H-89 was shown here. This disparity may have stemmed from differences between the cellular model and the use of cells as opposed to an organoid. The value of isoproterenol ED_{50} was observed in various studies, including beating rate in human embryonic stem cell-derived cardiomyocytes,[13] beating rate in human papillary

muscle strips of non-failing donor hearts,[14] and contractile force in hiPSC-CM-derived 3-dimensional engineered heart tissue. These findings indicate that similar concentrations of isoproterenol can impact the AC-cAMP/PKA cascade as well as PKA activity and other physiological processes in cardiomyocytes within multi-cellular *in-vitro* models and *ex vivo* human tissues. Examination of the tension of paced left atrial muscle preparations of male Hartley guinea pigs under increased concentrations of carbachol found an ED_{50} of 0.057 ± 0.014 μM.[15] This concentration is approximately one order of magnitude higher than the ED_{50} of carbachol for PKA activity in hiPSC-derived cardiac organoids. This difference may be due to the utilization of a different biological model or to the fact that the atrial muscle preparations were paced.

Spatial effect of drugs on PKA activity

Both direct modulation and sympathetic and parasympathetic stimulations of AC-cAMP/PKA cascade proteins, resulted in a heterogeneous 2D PKA response across cardiac organoid regions. This may be attributable to the unique internal structure of cardiac organoids, as previously demonstrated. Understanding the spatial dynamics of PKA activity within the complex architecture of cardiac organoids is essential for unraveling the regulatory mechanisms governing their behavior.

Forskolin and isoproterenol exerted a substantial spatial heterogenic effect on the cardiac organoid, with an almost 100% response measured for both, particularly at high concentrations. Conversely, H-89 and carbachol demonstrated a comparatively lower spatial heterogenic effect on the cardiac organoids, resulting in an approximate 50% response for both drugs at high concentrations. Comparison of drug pairs (forskolin and H-89, isoproterenol and carbachol), identified a statistically significant difference in their spatial effects. Therefore, the two activators of the AC-cAMP/PKA cascade elicited a higher response than the two inhibitors of the cascade.

In this study, we focused on spontaneously beating cardiac organoids. It is possible that PKA activity will differ in mature cardiomyocytes that do not spontaneously contract. Additionally, electrical pacing may result in contraction of specific parts of the organoid, which could, of course, affect spatiotemporal PKA activity. Future experiments will further characterize spatial contraction responses.

Conclusion

This work introduced, for the first time, measurement of PKA activity in cardiac organoids in response to modulation of the AC-cAMP/PKA cascade. Notably, the analysis extended beyond traditional 1D measurements at a single location and of the average PKA activity in a cardiac organoid over time, by providing a comprehensive 2D presentation capturing the spatial and temporal dynamics of PKA activity. The findings underscore the distinctive spatial impacts of substances targeting the AC-cAMP/PKA cascade, highlighting the distinct responses to activators and inhibitors. The insights promise to advance our understanding of the complex regulatory mechanisms within cardiac organoids, and inform future studies and applications in the field of cardiovascular research.

Limitations of the study

Our results apply to a single cell line. It has been speculated that drug responses in hiPSCs can be cell line-specific. However, in our previous work, the effects of forskolin and H-89 on Ca^{2+} transients and spontaneous beating rates were identical in two different cell lines.[8]

RESOURCE AVAILABILITY

Lead contact

Further information and requests for resources and reagents should be directed to and will be fulfilled by the lead contact, Prof. Yael Yaniv (yaely@bm.technion.ac.il).

Materials availability

This study did not generate new unique reagents.

Data and code availability

All data reported in this paper will be shared by the lead contact upon request. Any additional information required to reanalyze the data reported in this paper is available from the lead contact upon request.

ACKNOWLEDGMENTS

We thank Prof. Ofer Binah for the hiPSC cell line. This work was supported by the Israel Ministry of Science (Y.Y.) and the Rambam-Atidim Academic Excellence Program (W.-B.I.). The funders had no role in study design, data collection and analysis, decision to publish, or preparation of the manuscript.

Figure 1 and the graphical abstract were created with BioRender.com.

AUTHOR CONTRIBUTIONS

I.W.B. and Y.Y. wrote the manuscript. I.W.B. performed the cardiac organoid seeding and experiments with the assistance of S.M., R.E., and I.B. I.W.B. developed the data analysis algorithms and performed the data analysis. Y.Y. conceptualized, led, and supervised the project.

DECLARATION OF INTERESTS

The authors declare no competing interests.

STAR★METHODS

Detailed methods are provided in the online version of this paper and include the following:

- KEY RESOURCES TABLE
- EXPERIMENTAL MODEL AND STUDY PARTICIPANT DETAILS
  - hiPSC culture and differentiation to CM
- METHOD DETAILS
  - Cardiac organoid generation
  - Infection of a PKA cellular probe
  - Fluorescence signal acquisition
  - Fluorescence signal analysis
  - Regression calculation methods
  - Electrophysiological signal acquisition
  - Electrophysiological signal analysis
  - Immunofluorescence staining
  - Phospholamban phosphorylation activity measurement
- QUANTIFICATION AND STATISTICAL ANALYSIS

SUPPLEMENTAL INFORMATION

Supplemental information can be found online at https://doi.org/10.1016/j.isci.2025.112005.

Received: January 17, 2024
Revised: August 24, 2024
Accepted: February 10, 2025
Published: February 12, 2025

REFERENCES

1. Kim, H., Kamm, R.D., Vunjak-Novakovic, G., and Wu, J.C. (2022). Progress in multicellular human cardiac organoids for clinical applications. Cell Stem Cell *29*, 503–514.
2. Harvey, R.D., and Belevych, A.E. (2003). Muscarinic regulation of cardiac ion channels. Br. J. Pharmacol. *139*, 1074–1084.
3. Liu, Y., Chen, J., Fontes, S.K., Bautista, E.N., and Cheng, Z. (2021). Physiological And Pathological Roles Of Protein Kinase A In The Heart. Cardiovasc. Res. *118*, 386–398. https://pubmed.ncbi.nlm.nih.gov/33483740/.
4. Kirschner Peretz, N., Segal, S., Weiser-Bitoun, I., and Yaniv, Y. (2022). Distinct PKA Signaling in Cytosolic and Mitochondrial Compartments in Electrically Paced Atrial Myocytes. Cells *11*, 2261. https://www.mdpi.com/2073-4409/11/14/2261/htm.
5. Yaniv, Y., Ganesan, A., Yang, D., Ziman, B.D., Lyashkov, A.E., Levchenko, A., Zhang, J., and Lakatta, E.G. (2015). Real-time relationship between PKA biochemical signal network dynamics and increased action potential firing rate in heart pacemaker cells: Kinetics of PKA activation in heart pacemaker cells. J. Mol. Cell. Cardiol. *86*, 168–178.
6. Behar, J., Ganesan, A., Zhang, J., and Yaniv, Y. (2016). The autonomic nervous system regulates the heart rate through cAMP-PKA dependent and independent coupled-clock pacemaker cell mechanisms. Front. Physiol. *7*, 419.
7. Saucerman, J.J., Zhang, J., Martin, J.C., Peng, L.X., Stenbit, A.E., Tsien, R.Y., and McCulloch, A.D. (2006). Systems analysis of PKA-mediated phosphorylation gradients in live cardiac myocytes. Proc. Natl. Acad. Sci. USA *103*, 12923–12928. http://www.ncbi.nlm.nih.gov/entrez/query.fcgi?cmd=Retrieve&db=PubMed&dopt=Citation&list_uids=16905651.
8. Mazgaoker, S., Weiser-Bitoun, I., Brosh, I., Binah, O., and Yaniv, Y. (2023). cAMP-PKA signaling modulates the automaticity of human iPSC-derived cardiomyocytes. J. Gen. Physiol. *155*, e202213153. https://rupress.org/jgp/article/155/1/e202213153/213690/cAMP-PKA-signaling-modulates-the-automaticity-of.
9. Zhao, Z., Lan, H., El-Battrawy, I., Li, X., Buljubasic, F., Sattler, K., Yücel, G., Lang, S., Tiburcy, M., Zimmermann, W.-H., et al. (2018). Ion Channel Expression and Characterization in Human Induced Pluripotent Stem Cell-Derived Cardiomyocytes. Stem Cells Int. *2018*, 6067096.
10. Mandel, Y., Weissman, A., Schick, R., Barad, L., Novak, A., Meiry, G., Goldberg, S., Lorber, A., Rosen, M.R., Itskovitz-Eldor, J., and Binah, O. (2012). Human embryonic and induced pluripotent stem cell-derived cardiomyocytes exhibit beat rate variability and power-law behavior. Circulation *125*, 883–893. http://www.ncbi.nlm.nih.gov/entrez/query.fcgi?cmd=Retrieve&db=PubMed&dopt=Citation&list_uids=22261196.
11. Kitsuka, T., Itoh, M., Amamoto, S., Arai, K.I., Oyama, J., Node, K., Toda, S., Morita, S., Nishida, T., and Nakayama, K. (2019). 2-Cl-C.OXT-A stimulates contraction through the suppression of phosphodiesterase activity in human induced pluripotent stem cell-derived cardiac organoids. PLoS One *14*, e0213114.
12. Chijiwa, T., Mishima, A., Hagiwara, M., Sano, M., Hayashi, K., Inoue, T., Naito, K., Toshioka, T., and Hidaka, H. (1990). Inhibition of forskolin-induced neurite outgrowth and protein phosphorylation by a newly synthesized selective inhibitor of cyclic AMP-dependent protein kinase, N-[2-(p-bromocinnamylamino)ethyl]-5-isoquinolinesulfonamide (H-89), of PC12D pheochromocytoma. J. Biol. Chem. *265*, 5267–5272.
13. Brito-Martins, M., Harding, S.E., and Ali, N.N. (2008). β1- and β2-adrenoceptor responses in cardiomyocytes derived from human embryonic stem cells: comparison with failing and non-failing adult human heart. Br. J. Pharmacol. *153*, 751–759.
14. Bohm, M., Morano, I., Pieske, B., Ruegg, J.C., Wankerl, M., Zimmermann, R., and Erdmann, E. (1991). Contribution of cAMP-phosphodiesterase inhibition and sensitization of the contractile proteins for calcium to the inotropic effect of pimobendan in the failing human myocardium. Circ. Res. *68*, 689–701.
15. Chugun, A., Uchide, T., Fujimori, Y., Temma, K., Hara, Y., Sasaki, T., and Akera, T. (2000). Anti-muscarinic actions of mitoxantrone in isolated heart muscles of guinea pigs. Eur. J. Pharmacol. *407*, 183–189.
16. Depry, C., Allen, M.D., and Zhang, J. (2011). Visualization of PKA activity in plasma membrane microdomains. Mol. Biosyst. *7*, 52–58.
17. Lian, X., Zhang, J., Azarin, S.M., Zhu, K., Hazeltine, L.B., Bao, X., Hsiao, C., Kamp, T.J., and Palecek, S.P. (2013). Directed cardiomyocyte differentiation from human pluripotent stem cells by modulating Wnt/β-catenin signaling under fully defined conditions. Nat. Protoc. *8*, 162–175. https://pubmed.ncbi.nlm.nih.gov/23257984/.
18. Schafer, R. (2011). What is a savitzky-golay filter? IEEE Signal Process. Mag. *28*, 111–117.
19. Hill, A.V. (1910). The possible effects of the aggregation of the molecules of haemoglobin on its dissociation curves. J Physiol. *40*. iv-vii.

STAR★METHODS

KEY RESOURCES TABLE

REAGENT or RESOURCE	SOURCE	IDENTIFIER
Bacterial and virus strains		
pcDNA3-A-kinase activity receptor 4 (AKAR4) cytosolic fluorescence resonance energy transfer (FRET)-based PKA probe	Depry, Allen and Zhang[6]	pcDNA3-AKAR4, Addgene ID 61619
Chemicals, peptides, and recombinant proteins		
Corning® Matrigel® Growth Factor Reduced (GFR) Basement Membrane Matrix, Phenol Red-free	GFR, BD Biosciences	Product Number 356231
mTeSR™1	Stemcell Technologies	Catalog #85850
Versene Solution	Thermo Fisher Scientific	Catalog number: 15040066
TrypLE™ Express Enzyme (1X), no phenol red	Thermo Fisher Scientific	Catalog number: 12604013
DMEM, high glucose	Thermo Fisher Scientific	Catalog number: 41965039
Gibco™ Fetal Bovine Serum, qualified, Brazil	Fisher Scientific	Product Code.11573397
Fetal Bovine Serum (FBS), Qualified for Human Embryonic Stem Cells	Biological Industries	Model 04-002-1A
MEM Non-Essential Amino Acids Solution (100X)	Thermo Fisher Scientific	Catalog number: 11140050
GlutaMAX™ Supplement	Thermo Fisher Scientific	Catalog number: 35050038
Penicillin-Streptomycin Solution	SARTORIUS	SKU 03-031-1B
Paraformaldehyde	Electron Microscopy Sciences	SKU 15710
Triton X-100	Sigma-Aldrich	Product Number 93443-100ML
PBS pH 7.4 (10X)	Gibco	70011036
DAPI	Sigma-Aldrich	Product Number D9542
Anti-Troponin I Antibody, a.a. 186-192, clone C5	Sigma-Aldrich	MAB1691
Anti-HCN4 antibody	Abcam	ab66501
Phospholamban (PLN, PLB) (pSer16) pAb serum	Badrilla	Product code A010-12
Donkey Anti-Mouse IgG H&L (Alexa Fluor® 488) preadsorbed (ab150109)	Abcam	ab150109
Anti-Rabbit-IgG - Atto 647N antibody produced in goat,1 mg/mL IgG Sigma-Aldrich 40839-1ML-F	Sigma-Aldrich	40839
F(ab')2 Goat anti Rabbit IgG (H+L) Secondary Antibody, Alexa Fluor 488	Invitrogen	Catalog # A-11070
35 mm Dish | No. 1.0 Coverslip 14 mm Glass Diameter | Uncoated	MatTek Corporation	Part No: P35G-1.0-14-C
Experimental models: Cell lines		
Human induced pluripotent stem (hiPS) cell line	Depry et al.[16]	hiPS cell line no. 24.5
Software and algorithms		
MATLAB	The MathWorks, Inc.	2022b
Other		
pluriStrainer Mini 100 μm (Cell Strainer)	pluriSelect	SKU 43-10100-40
Microelectrode Array	Multi-Channel System	60MEA100/10iR-ITO-gr

EXPERIMENTAL MODEL AND STUDY PARTICIPANT DETAILS

hiPSC culture and differentiation to CM

A hiPSC line derived from a skin biopsy obtained from a 46-year-old female volunteer, as detailed in a previous study (Novak et al., 2015), served as the cell source. The donor provided informed consent in accordance with the guidelines set forth by the Helsinki Committee for experiments on human subjects at Rambam Health Care Campus, Haifa, Israel (approval #3116). The hiPSCs were cultured on Matrigel (GFR, BD Biosciences, Franklin Lakes, NJ, USA)-coated plates and maintained in a 5% CO_2 incubator (Forma series 3 water jacketed CO_2 incubator, Thermo Scientific, MA, USA) at 37°C. Cells were maintained in mTesR1 cell culture medium (Stemcell Technologies, Vancouver, Canada) and dissociated and recultured in Versene (Thermo Fisher Scientific, Waltham, MA, USA). For cardiac differentiation, the Wnt/β-catenin signaling modulation protocol was applied, as previously described.[17]

METHOD DETAILS

Cardiac organoid generation

CMs were dissociated 29-64 days after differentiation initiation (Table S1) by adding 0.5 ml per well (in a 12-well plate) of TrypLE (Thermo Fisher Scientific), followed by an 8-min incubation at 37°C in a 5% CO_2 incubator. The cells were gently pipetted with 1 ml embryonic body (EB) medium comprised of DMEM (Thermo Fisher Scientific), supplemented with 20% (w/w) fetal bovine serum (Gibco), 1% (w/w) MEM Non-Essential Amino Acids Solution (Thermo Fisher Scientific), 1% (w/w) GlutaMax (Thermo Fisher Scientific), and 1% (w/w) PenStrep (Biological Industries). The well was washed twice with an additional 1 ml of EB medium. Cells and medium were collected into a conical tube and diluted in an additional 9 ml EB medium. To ensure cell dissociation, the cells were passed through a 100 μm cell strainer (pluriSelect), and the resulting cell suspension was centrifuged (Spectrafuge 6C, Labnet) for 5 min, at 1500 rpm. After aspirating the supernatant, the cell pellet was seeded onto Matrigel-coated 35 mm dishes (MatTek Corporation). To optimize the seeding area, cells were seeded inside a custom-made seeding-guide ring with a 1 mm^2 hole area, which was placed on the dish. Dishes were then incubated at 37°C in a 5% CO_2 incubator. On the day following cell seeding, the ring was removed, and organoid culture was continued for an additional 5-6 days with EB medium replacement every 2-3 days. Organoids were generated from at least three different CM differentiation batches, differentiated from hiPSCs of passage number up to 45.

The organoid showed clear sarcomere formation (Figure S1) and propagation of electrical activity (Figure S2).

For multi-electrode array (MEA) measurements, cells were seeded onto MEA plates (60MEA100/10iR-ITO-gr, Multi-Channel System, Germany). To optimize the seeding area, cells were seeded inside a custom-made seeding-guide ring with a 1.5 mm^2 hole, which was placed onto the plates. The ring was removed one day following cell seeding.

Infection of a PKA cellular probe

At 7-8 days post-seeding, organoids were infected with adenoviral particles containing a pcDNA3-A-kinase activity receptor 4 (AKAR4) cytosolic fluorescence resonance energy transfer (FRET)-based PKA probe, as previously described.[16] The PKA biosensor-containing plasmids were generated by Vector Biolabs (Malvern, Pennsylvania, USA). A viral concentration of $4.2x10^6$ infectious units per milliliter (IFU/ml) ($15x10^7$ viral particles per milliliter, VP/ml) was utilized. The fluorescence signal was measured on the following day.

Fluorescence signal acquisition

Before imaging, the EB medium was aspirated, and spontaneously beating organoids were rinsed twice with Tyrode's solution comprised of (in mM): 140 NaCl, 5.4 KCl, 10 glucose, 1 $MgCl_2$, 2 sodium pyruvate, 10 HEPES, and 2 $CaCl_2$. The pH was adjusted to 7.4 using NaOH. This solution was also employed as the imaging medium during the imaging process.

Real-time FRET imaging was performed under heating control conditions to maintain the sample at 37°C, with an LSM880 confocal microscope (Zeiss, Oberkochen, Germany) equipped with a 10x/0.45 lens. A 405 nm excitation light source was utilized. This biosensor comprises the simultaneous measurement of cyan fluorescent protein (CFP) and yellow fluorescent protein (YFP) emissions within the ranges of 460-500 nm and 520-585 nm, respectively, and were collected using a 458/514 nm mirror beam splitter. A total of 256x256 pixel images were recorded at a rate of 3.14 Hz. Each experimental step, whether control or involving a specific drug, captured 1000 frames for each channel (CFP and YFP). Subsequently, the next drug was introduced into the dish, followed by a 10-minute incubation without imaging to allow for the stabilization of its effect on the FRET signal. Drugs were added manually with a pipette to avoid perfusion that could affect the spatiotemporal activation of PKA.

Fluorescence signal analysis

Time-series fluorescence images were analyzed using a custom-made MATLAB platform named "PhysioFluo", designed for fluorescence data analysis in physiological experiments (MATLAB 2022b, The MathWorks, Inc.). Background intensity outside the organoid contour was subtracted from each image of each channel during each experimental step, to account for changes in the background throughout the measurement. Image down-resolution was implemented to reduce random noise, resulting in 10x10 pixel images. The FRET time-series data were computed by dividing the YFP and CFP emissions (FRET signal = YFP/CFP) for each corresponding pixel, generating two-dimensional FRET images over time, with a 10x10 spatial resolution (i.e., 100 time-series signals per

experimental step). The FRET data were normalized by the mean baseline FRET data of each location and filtered using a Savitzky-Golay filter with a polynomial order of 5 and a frame length of 51.[18] This process resulted in normalized YFP/CFP signals that were further employed for analysis.

The mean FRET signal for each location in each experimental step was calculated. To identify the representative location for substance activity in each organoid, each location was graded based on its FRET response to all substance concentrations, enabling quantification of the response trend across all locations. Only locations that responded to drugs were used for calculations of PKA variability among different areas.

By measuring blank (baseline) samples, it was determined that there was no significant decay in the FRET data over seven measurements (representing the maximum number of steps used for substance measurements), as illustrated in Figure S5.

Regression calculation methods

To compute the regression of the PKA response, the initial step involved calculation of the difference in the local normalized YFP/CFP signal for each cardiac organoid in relation to the baseline signal for all tested drugs.[19] Subsequently, the regression of the data corresponding to all concentrations of each substance (forskolin at 0.1, 1, 10, and 100 μM; H-89 at 0.1, 1, and 10 μM; isoproterenol at 1, 10, 100, and 1000 nM; carbachol at 1, 10, 100, and 1000 nM) was carried out using the Hill equation: $\left(\Delta\frac{F_{YFP}}{F_{CFP}} = \frac{a}{1+\left(\frac{b}{Conc.}\right)^{n}}\right)$.

For each cardiac organoid, R^2 and the effective dose for 50% response (ED_{50}) were determined as part of the regression analysis.

Electrophysiological signal acquisition

Two days post-seeding, the EB medium was aspirated from the MEA plates, and spontaneously beating cardiac organoids were rinsed with 1 ml Tyrode's solution. This solution was also employed as the medium during the measurement process. Electrical activity was measured with a MEA recording system (MEA1060-INV-BC, Multi-Channel System, Germany), at a sampling frequency of 10,000 Hz and under temperature control (TC01/02, Multi-Channel System, Germany) to maintain the sample in 37°C. The data from all sixty electrodes were recorded simultaneously. In order to reduce noises and to ground the MEA plate, a reference electrode (Ag/AgCl-pellet, Multi-Channel System, Germany) was connected to the MEA recording device and its edge was inserted into the MEA plate filled with the Tyrode's solution.

Electrophysiological signal analysis

The electrical (voltage) activity of the cardiac organoids was analyzed using a custom-made MATLAB platform named "PhysioMEA", designed for MEA data analysis of physiological experiments (MATLAB 2023b, The MathWorks, Inc.). After applying a notch filter (to remove the electric frequency) and moving average filter (to remove random noise), the R-peaks were detected. The electrical signal is presented as measured from one electrode on Figure S2.

Immunofluorescence staining

Cardiac organoids seeded onto Matrigel-coated 35 mm dishes were fixed with 4% paraformaldehyde (Electron Microscopy Sciences, PA, USA, diluted in PBS) for 20 min, at room temperature. They were then washed three times with PBS pH 7.4 (10X) (Gibco) diluted 1:10 in ddH_2O and permeabilized with 1% Triton X-100 (Sigma-Aldrich, diluted in PBS) for 10 min at room temperature. Organoids were blocked with 5% fetal bovine serum (Gibco, diluted in PBS) and incubated overnight at 4°C with primary antibodies diluted in antibody buffer comprised of PBS with 10% of 1% Triton and 3% fetal bovine serum. The following day, organoids were washed three times and incubated with conjugated secondary antibodies diluted in antibody buffer for 1 h, at room temperature, in the dark. Organoids were washed three times and DAPI was applied (Sigma-Aldrich) to stain the nuclei.

Primary antibodies used included anti-troponin I antibody (Sigma-Aldrich, 1:200) and anti-hyperpolarization-activated channel 4 (HCN4) antibody (Abcam, 1:500). Secondary antibodies used included Alexa Fluor 488-conjugated donkey anti-mouse IgG antibody (Abcam, 1:200) and Atto 647N-conjugated anti-rabbit IgG antibody (Sigma-Aldrich, 1:200), respectively.

Samples were viewed with an inverted Eclipse Ti-E confocal microscope with a spinning disk (Nikon Instruments Inc., Melville, NY, USA) equipped with a 20x/0.45 lens. A total of 1024x1024 pixel fluorescence images were recorded.

Phospholamban phosphorylation activity measurement

EB medium was aspirated from cardiac organoid dishes, which were then rinsing twice with Tyrode's solution. Plates were incubated at 37°C in Tyrode's solution for at least 30 min. Organids were then further incubated (for control and negative control conditions) or treated with 10 μM FSK or H-89 for 15 min and immediately stained as described above. Phosphorylated phospholamban (pSER16) pAb serum (Badrilla, 1:200) diluted in antibody buffer was used as a primary antibody. For negative control, cardiac organoids were treated with antibody buffer only. Alexa Fluor 488 goat anti-rabbit IgG antibody (Invitrogen, 1:200) was used as a secondary antibody.

Imaging was performed with a LSM880 confocal microscope (Zeiss, Oberkochen, Germany) equipped with a 10x/0.45 lens and a 488 nm excitation light source. Emission within the range of 493-630 nm.

Fluorescence images (4096x4096 pixel) were analyzed using ''PhysioFluo'' (MATLAB 2023b, MathWorks, Inc.). Background intensity outside the organoid contour was subtracted from each image. To calculate the mean signal of each image and avoid averaging regions without organoid cells, pixels with the top 80% of fluorescence intensity were utilized to calculate the mean phosphorylated phospholamban signal. The normalized mean signal was calculated by dividing the mean signal of each image by the mean signal of the control organoid images.

QUANTIFICATION AND STATISTICAL ANALYSIS

The analyzed data were computed and presented as mean ± standard error (SE). To compare the dose-response of substances, a one-way analysis of variance (ANOVA) was employed. Additionally, a two-sample t-test was utilized for the comparison of two drugs. results were deemed statistically significant for p values < 0.05; p values are explicitly indicated in the figures for reference.